PHYSICAL REVIEW A **68**, 031404(R) (2003)

Unexpected instabilities in the dynamic Kingdon trap

I. Garrick-Bethell[1] and R. Blümel[2]
[1]*MIT Center for Space Research, Cambridge, Massachusetts 02139, USA*
[2]*Department of Physics, Wesleyan University, Middletown, Connecticut 06459-0155, USA*
(Received 8 July 2003; published 25 September 2003)

We report the discovery of unexpected instabilities of a trapped charged particle in the dynamic Kingdon trap. A detailed phase-space analysis shows that these instabilities are caused by the collapse of the primary trapping island. A resonance condition accurately predicts the locations of the instabilities. Avoiding these instabilities is essential for successfully operating the dynamic Kingdon trap.

DOI: 10.1103/PhysRevA.68.031404 PACS number(s): 32.80.Pj

The storage of charged particles in ion traps is of growing interest in contemporary physics. Ion trapping was pioneered by Paul and Dehmelt who won a Nobel Prize each for their contributions to the field [1,2]. Nowadays ion traps are employed both in fundamental and applied research ranging from the implementation of quantum computing schemes [3] to the investigation of antimatter [4,5]. The two workhorses of these investigations are the Paul trap [1,6] and the Penning trap [2,6]. Both traps rely on electric quadrupole fields, in the case of the Penning trap supplemented with a magnetic field, to achieve charged particle trapping. A relative newcomer to the field of charged particle trapping is the dynamic Kingdon trap [7] which relies on a superposition of static and time-varying electric monopole fields. It is also a member of a class of ''wire traps'' which have been investigated intensively during the past decade for the trapping of neutral particles [8–10].

A sketch of the dynamic Kingdon trap is shown in Fig. 1. The trap consists of a rectilinear conducting wire surrounded by a cylindrical conducting surface. A combination of dc and ac voltages is applied between the central wire and the conducting cylinder. The trap derives its name from the static version of this device which was reported by Kingdon [11]. Unlike the static trap the dynamic Kingdon trap allows stable particle confinement in the radial direction even if the particle's angular momentum is zero [7]. Trapping in the axial direction may be achieved by using end caps [7]. The dynamic Kingdon trap was originally developed in the late 1960s [12] and early 1970s [13] as a mass selective ion source. It was rediscovered in the mid 1990s [7] as a micro laboratory for the investigation of classical and quantum chaos [14]. The trap's classical dynamics has been studied in detail [7,15–18] and experimental implementations [12,13,19,20] demonstrated that this device is indeed capable of trapping charged particles under laboratory conditions.

In the following we analyze the classical dynamics of the radial motion of a single trapped charged particle with charge Q, mass m, and zero angular momentum. For simplicity we will assume an ideal cylindrical device. This is not an oversimplification, since it was shown [7] that even in the presence of end caps the motion of a trapped particle is still described to a good approximation by the equations of motion of the ideal cylindrical trap.

Applying a combination of a dc and an ac voltage of frequency Ω to the trap generates a linear charge density $\sigma(t)=\sigma_{\rm dc}-\sigma_{\rm ac}\cos(\Omega t)$ on the wire. The polarity of the dc voltage has to be chosen such that the trapping condition [7] $Q\sigma_{\rm dc}<0$ is fulfilled. Using Gauss' theorem [21] it is then straightforward to show [15] that the equation of motion of the trapped particle in the radial direction is given by

$$\frac{d^2\rho}{d\tau^2}+[1-2\eta\cos(2\tau)]\frac{1}{\rho}=0, \tag{1}$$

where ρ is the dimensionless radial coordinate of the particle in units of $l=[-2Q\sigma_{\rm dc}/\pi\epsilon_0 m\Omega^2]^{1/2}$, ϵ_0 is the electric permittivity of the vacuum, $\tau=\Omega t/2$ is dimensionless time, and $\eta=\sigma_{\rm ac}/2\sigma_{\rm dc}$ is the dimensionless control parameter. The properties of Eq. (1) are independent of the sign of η, so that without restriction of generality we focus on the case $\eta>0$. Note that although the dc and ac voltages may be chosen independently, the scaled equation of motion (1) depends only on the single control parameter η.

The equation of motion (1) is nonlinear and difficult to analyze exactly. An approximate method, however, provides valuable insight into the trapping mechanism. Using the method of averaging [22] it can be shown [7,15,16] that to a good approximation the trapped charged particle experiences the effective time-averaged pseudopotential [23]

$$V_{\rm eff}(\rho)=\ln(\rho)+\frac{\eta^2}{4\rho^2}. \tag{2}$$

This potential has a minimum at $\rho_M=\eta/\sqrt{2}$ and rises monotonically and globally to both sides of ρ_M. Therefore, based on the pseudopotential approach one is led to conclude that trapping is stable for all control parameters η. This, however, is not so [24]. Going beyond the pseudopotential ap-

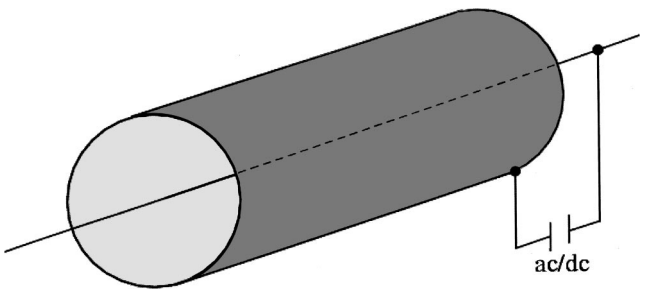

FIG. 1. Sketch of the dynamic Kingdon trap.

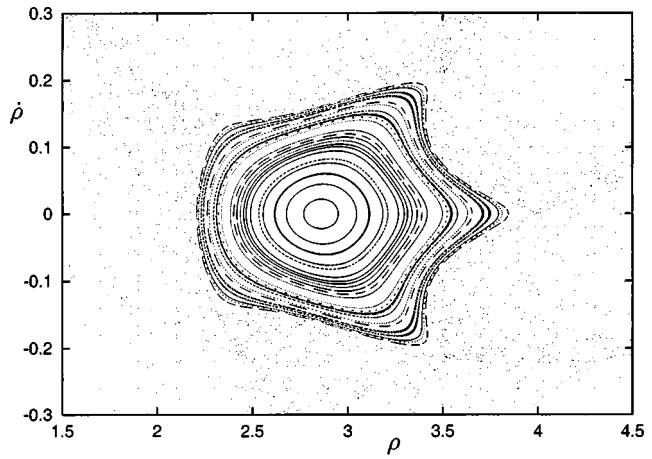

FIG. 2. Primary trapping island for $\eta=5$.

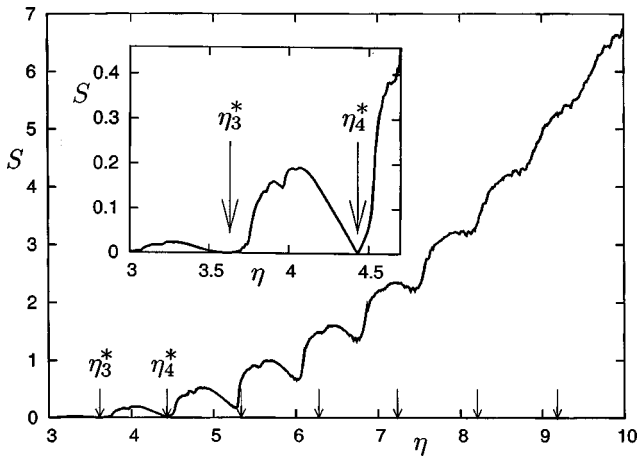

FIG. 3. The stability function $S(\eta)$ as a function of the control parameter η. The inset shows that $S(\eta)$ vanishes at $\eta_3^*\approx 3.61$ and $\eta_4^*\approx 4.43$ (marked by arrows), indicating instability of the dynamic Kingdon trap at η_3^* and η_4^*. The arrows for $\eta>\eta_4^*$ mark the η values where the rotation frequency of the center of the trapping island is in resonance with the frequency of the trap's ac voltage.

proximation by directly analyzing Eq. (1) both numerically and analytically, we discovered two η values where the trap is unstable. In addition, we found several η values where the trap exhibits reduced stability. We now prove these facts and reveal the origin of the instabilities in the dynamic Kingdon trap.

The best way to illustrate the trapping mechanism of the dynamic Kingdon trap is by means of a strobed phase-space plot. Starting at a phase-space point $(\rho,\dot{\rho})$, where $\dot{\rho}\equiv d\rho/d\tau$, we integrate Eq. (1) over one cycle of the ac voltage forward in time and obtain the phase-space point $(\rho',\dot{\rho}')$. The integration over one cycle defines a mapping $(\rho,\dot{\rho})\rightarrow(\rho',\dot{\rho}')$ of the phase space onto itself, which we call the ''Kingdon mapping.'' To illustrate the method, we solved Eq. (1) for $\eta=5$ and 256 initial conditions $[\rho_i(\tau=0)=1.5+(i-1)\times 0.2, \dot{\rho}_j(\tau=0)=-0.3+(j-1)\times 0.04$, where $i,j=1,\ldots,16]$ and plotted $(\rho_i(\tau_k),\dot{\rho}_j(\tau_k))$ for each (i,j) combination at the 500 discrete times $\tau_k=k\pi$, $k=1,\ldots,500$. The resulting phase-space portrait (see Fig. 2) shows that the phase space is dominated by a single large regular island surrounded by a chaotic sea. Trajectories that started inside the island stay trapped inside the island forever. Therefore we call the island shown in Fig. 2 the primary trapping island. Apart from a small set of trajectories launched at special initial conditions, most trajectories that started outside the island, after a brief chaotic transient, either reach the outer cylindrical electrode or the axial wire. In both cases the particle discharges and is lost from the trap. The location $\rho_C(\eta)$ of the center of the primary trapping island in Fig. 2 is consistent with [7,18]

$$\rho_C(\eta)\approx\frac{\eta-1}{\sqrt{2}}, \tag{3}$$

which predicts $\rho_C\approx 2.83$ at $\eta=5$.

For some values of η small secondary trapping islands surround the primary trapping island like satellites. Since the sum total $S(\eta)$ of the phase-space area of all stable islands determines the storage efficiency, $S(\eta)$ is a fundamental characteristic function of the trap. For given η we determine $S(\eta)$ by (i) producing a detailed phase-space portrait (see, for example, Fig. 2), (ii) visually inspecting the portrait, (iii) determining a rectangular window $W(\eta)$ that encloses all regular regions of phase space, (iv) covering the window uniformly with a regular grid of 40 000 phase-space points P_k, $k=1,\ldots,40\,000$, with spacings $\Delta\rho<0.04$, $\Delta\dot{\rho}<0.004$ (the exact spacings depend on the size of $W(\eta)$, but are always small enough to ensure convergence), (v) iterating every single one of the starting points P_k forward in time for 1 000 cycles of the trap field, (vi) counting the number $N(\eta)$ of the P_k's whose iterates never leave $W(\eta)$, and (vii) computing $S(\eta)$ according to $S(\eta)\approx N(\eta)\times\Delta\rho\times\Delta\dot{\rho}$. We used this scheme to evaluate $S(\eta)$ with a resolution of $\Delta\eta=0.01$ from $\eta=3$ to $\eta=10$ at the mesh points $\eta^{(n)}=3+(n-1)\Delta\eta$, $n=1,\ldots,701$. The result is shown in Fig. 3. The inset shows that $S(\eta)$ vanishes at $\eta\approx 3.61$ (labeled η_3^*) and at $\eta\approx 4.43$ (labeled η_4^*), and shows pronounced dips at several other η values. This result implies that the dynamic Kingdon trap is unstable at η_3^* and η_4^*. On the basis of pseudopotential theory this result is completely unexpected.

Analyzing the phase-space structures in the vicinity of η_3^* reveals the origin of the instabilities and explains our notation for their locations. Figure 4 shows a sequence of three phase-space plots for $\eta=3.576$ [Fig. 4(a)], $\eta=3.613$ [Fig. 4(b)], and $\eta=3.650$ [Fig. 4(c)]. Figure 4(a) shows that close to η_3^* the primary trapping island is caged by a triangle whose vertices are unstable period-3 fixed points of the Kingdon mapping. Period-3 means that starting the trapped particle with phase-space coordinates at one vertex of the triangle, the phase-space coordinates of the particle visit the other two vertices after one and two trap cycles, respectively, before returning to the starting vertex. Since, as shown in Fig. 4(a), the unstable period-3 fixed points render the outside of the caging triangle chaotic, the interior of the triangle,

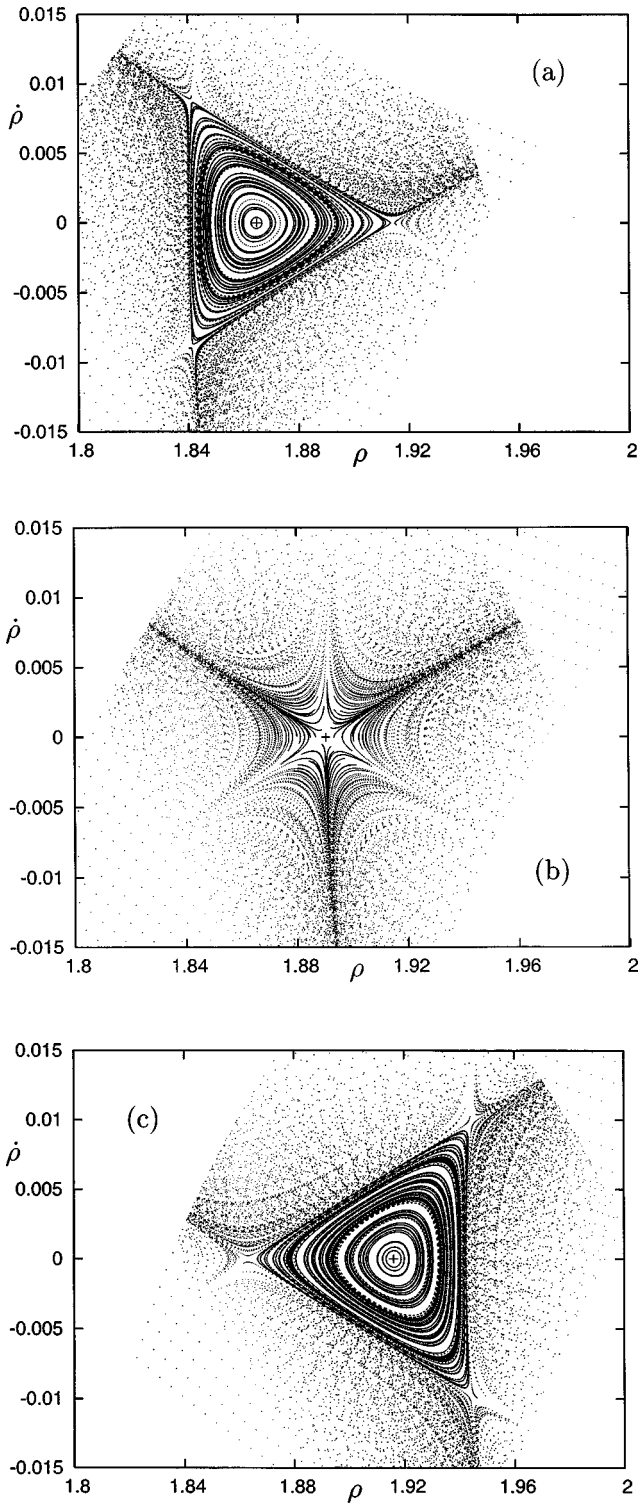

FIG. 4. Illustration of island collapse in the vicinity of $\eta = \eta_3^*$. (a) $\eta = 3.576$, (b) $\eta = 3.613 \approx \eta_3^*$, and (c) $\eta = 3.650$. The center of the primary trapping island is marked by the plot symbol $+$. It shifts to the right in accordance with Eq. (3).

containing the primary trapping island, is the largest stable region of phase space. Our computations show that approaching $\eta = \eta_3^*$ the triangle becomes smaller, squeezing the primary trapping island to ever smaller sizes. Figure 4(b) shows that at $\eta = \eta_3^*$ the triangle collapses to a point, squeezing the primary trapping island to zero area. We call this process ''island collapse.'' Figure 4(c) shows that for η larger than η_3^* the caging triangle reemerges and with it the primary trapping island. Thus the reason for the instability of the dynamic Kingdon trap at η_3^* is revealed: it is due to the complete elimination of the primary trapping island at η_3^* by a collapsing set of period-3 fixed points. At η_3^* the center of the primary trapping island and the period-3 fixed points degenerate into a single point. This picture also explains the subscript ''3'' we chose to label the η value where the island collapse occurs. We note that the center of the primary trapping island, marked by a $+$ in Fig. 4, shifts to the right from frames (a) to (c). This is expected and predicted according to Eq. (3). Denoting by $\Delta\rho_C$ the shift of the center of the trapping island, we obtain from Eq. (3) $\Delta\rho_C \approx \Delta\eta/\sqrt{2} \approx 0.0524$, which is in good agreement with $\Delta\rho_C \approx 0.051$ extracted from Fig. 4.

Island collapse leads to a resonance condition that has to be fulfilled at the point of collapse. Since it takes three trap cycles to revolve once through the vertices of the caging triangle, the outer boundary of the primary trapping island, hugging the sides of the caging triangle, revolves at a frequency of close to $\Omega/3$ around the central period-1 fixed point. This means that close to the collapse point the winding frequency of the primary trapping island is nearly in resonance (an approximate 1:3 resonance) with the trap frequency. At the collapse point $\eta = \eta_3^*$ the resonance is exact.

Our calculations show that a similar process takes place at $\eta = \eta_4^*$. This time a period-4 fixed point in the shape of a rectangle cages the primary trapping island. Total island collapse is observed at $\eta = \eta_4^*$.

Figure 3 shows reduced stability at $\eta \approx$ 5.28, 6.01, 6.74, 7.45, and 8.08. In these cases higher-order polygons cage the primary trapping island. Island collapse, however, is incomplete in these cases, since the polygons do not completely collapse. Still, as shown by Fig. 3, the incomplete collapse manifests itself in dips in $S(\eta)$, whose depths reflect the degree of the partial island collapse.

The resonance mechanism allows us to accurately predict the positions of island collapse. Let us denote by ω the scaled winding frequency of the primary trapping island. According to Eq. (1) a 1:1 resonance with the driving frequency corresponds to $\omega = 2$. Therefore a 1:3 resonance, as required in the vicinity of η_3^*, is obtained for $\omega = 2/3$. For given η we determine the winding frequency in the following way. We denote the time evolution of the period-1 fixed point of the Kingdon mapping during a mapping cycle by $\rho_f(\tau)$. Since we are interested in the situation of very small island sizes close to the critical control parameters η_3^* and η_4^*, we linearize the equation of motion (1) around $\rho_f(\tau)$, obtaining

$$\ddot{\xi}(\tau) - [1 - 2\eta\cos(2\tau)]\frac{\xi(\tau)}{\rho_f^2(\tau)} = 0, \tag{4}$$

where we defined $\rho(\tau) = \rho_f(\tau) + \xi(\tau)$ and expanded Eq. (1) to first order in ξ. Solving Eq. (4) over one cycle of the trap's

driving voltage, we obtain the linear phase-space mapping $(\xi', \dot{\xi}') = M(\eta)(\xi, \dot{\xi})$, where $M(\eta)$ is a 2×2 matrix with time-independent matrix elements that depend only on the control parameter η. Since close to the center of the primary trapping island $M(\eta)$ describes a rotation, its eigenvalues $\lambda(\eta)$ are of the form $\lambda_{1,2}(\eta) = \exp[\pm i\omega(\eta)\pi]$ [25], where $\omega(\eta)$ is the winding frequency of the primary trapping island. All we have to do now is to solve the equations $\omega(\eta) = 2/3$ and $\omega(\eta) = 2/4 = 1/2$. We obtain $\eta_3^* = 3.613\,046\,7\ldots$ and $\eta_4^* = 4.431\,124\,4\ldots$, consistent with the collapse positions in Fig. 3.

For incomplete island collapse the synchronization of the primary trapping island with the caging polygon is not complete and the resonance criterion works only approximately. This happens for $\eta > \eta_4^*$ where the resonance conditions $\omega(\eta) = 2/5$, 2/6, 2/7, 2/8, and 2/9 have solutions $\eta \approx 5.3351$, 6.2759, 7.2335, 8.2031, and 9.1798, respectively. They are marked by the arrows in Fig. 3. As expected, the agreement of resonance values (arrows) with the locations of the minima of $S(\eta)$ is not too good, and gets worse as the dips of $S(\eta)$ get shallower, indicating progressively incomplete island collapse. Agreement is best for the first dip at $\eta \approx 5.3$, where the collapse of the primary trapping island is nearly complete.

We found that island collapse also occurs for other types of traps. For example, a charged particle trapped in the spherical dynamic Kingdon trap [17] is described by the equation of motion $\ddot{\rho} + [1 - 2\eta\cos(2\tau)]/\rho^2 = 0$ and shows island collapse at $\eta \approx 3.16$ and $\eta \approx 3.86$ [24]. Thus island collapse seems to be a generic property of electrodynamic monopole traps.

Although its roots go back more than 30 years, the development of the dynamic Kingdon trap was temporarily suspended in the mid 1970s because of instabilities, which were not well understood at the time [26]. It is possible that the instabilities discussed in this paper have something to do with the instabilities that contributed to the premature cancellation of the early successful Kingdon research program at Freiburg University [12,13]. In any case, knowledge of these instabilities is essential for successfully operating the dynamic Kingdon trap.

The authors gratefully acknowledge financial support by NSF Grant No. PHY-9984075.

[1] W. Paul, Rev. Mod. Phys. **62**, 531 (1990).
[2] H. Dehmelt, Rev. Mod. Phys. **62**, 525 (1990).
[3] J.I. Cirac and P. Zoller, Phys. Rev. Lett. **74**, 4091 (1995).
[4] G. Gabrielse *et al.*, Phys. Rev. Lett. **89**, 213401 (2002).
[5] M. Holzscheiter *et al.*, Hyperfine Interact. **109**, 1 (1997).
[6] P.K. Ghosh, *Ion Traps* (Clarendon Press, Oxford, 1995).
[7] R. Blümel, Phys. Rev. A **51**, R30 (1995).
[8] R. Blümel and K. Dietrich, Phys. Rev. A **43**, 22 (1991).
[9] M. Müller and K. Dietrich, Phys. Rev. A **54**, 2577 (1996).
[10] A. Haase, D. Cassettari, B. Hessmo, and J. Schmiedmayer, Phys. Rev. A **64**, 043405 (2001).
[11] K.H. Kingdon, Phys. Rev. **21**, 408 (1923).
[12] R.E. Bahr, Diplomarbeit, Physikalisches Institut der Universität Freiburg, 1969 (unpublished).
[13] E. Behre, Zulassungsarbeit, Physikalisches Institut der Universität Freiburg, 1972 (unpublished).
[14] M.C. Gutzwiller, *Chaos in Classical and Quantum Mechanics* (Springer, New York, 1990).
[15] R. Blümel, Phys. Scr. **T59**, 126 (1995); **T59**, 369 (1995).
[16] R. Blümel, Appl. Phys. B: Lasers Opt. **60**, 119 (1995).
[17] R. Blümel, E. Bonneville, and A. Carmichael, Phys. Rev. E **57**, 1511 (1998).
[18] S.J. Linz, Phys. Rev. A **52**, 4282 (1995).
[19] E. Peik and J. Fletcher, J. Appl. Phys. **82**, 5283 (1997).
[20] N. Yu and H. Dehmelt, in *Trapped Charged Particles and Fundamental Physics*, edited by D.H.E. Dubin and D. Schneider, AIP Conf. Proc. No. 457 (AIP, Woodbury, NY, 1999) p. 261.
[21] J.D. Jackson, *Classical Electrodynamics* (Wiley, New York, 1975).
[22] L.D. Landau and E.M. Lifshitz, *Mechanics* (Pergamon, Oxford, 1960).
[23] H.G. Dehmelt, Adv. At. Mol. Phys. **3**, 53 (1967).
[24] I. Garrick-Bethell, Senior thesis, Wesleyan University, 2002 (unpublished).
[25] J. Guggenheimer and P. Holmes, *Nonlinear Oscillations, Dynamical Systems, and Bifurcations of Vector Fields* (Springer, New York, 1983).
[26] E. Teloy (private communication).